# TRANSPORT AND CHEMICAL EVOLUTION OF YELLOW SAND IN KOREA

Byung-Gon Kim

*Air Quality Research Department*
*National Institute of Environmental Research*
*Kyungseodong Seogu, Inchun 404-170, Korea*

## 1. INTRODUCTION

Asian dust what is called 'Huang sha' in Chinese, 'Whangsa' in Korean, and 'Kosa' in Japanese, can be transported thousands of kilometers over Korea, Japan, and out into the Pacific Ocean (Iwasaka et al., 1983). The Yellow Sand (YS) phenomenon observed in the Korean peninsula originates mainly from the Takla-Makan Desert, the Gobi Desert and the Loess Plateau of China. Central Asia is one of the world's largest dust sources, however, the magnitude of this source remains highly uncertain but is to be of the order of 800 Tg $yr^{-1}$ (Zhang et al., 1997). The production and long-range transport of mineral dust from the Asian continent impact atmospheric chemistry and the radiative balance over a large region, and affect biological productivity in the North Pacific Ocean (Gao et al., 1992). Atmospheric aerosols are important components of the earth-atmosphere system, which play a major role in both the global climate and in many biogeochemical cycles. Aerosols also help control the concentration, life time and the physical and chemical behavior of many important tracer gases, such as sulfur, nitrogen, and carbon by providing reaction sites and serving as carriers and/or sinks for many atmospheric species (Zhang and Carmichael, 1999; Dentener et al., 1996).

Mineral dust also has the potential to modify gas-phase chemistry by absorbing acidic gases such as $SO_2$ and NOx, which is then oxidized to sulfate and nitrate (Dentener et al., 1996; Xiao et al., 1997; Kim and Park 2001). Yet few of these effects can be quantified adequately, in part due to a lack of comprehensive observations over time in source regions.

YS phenomena are generally observed 0-6 times per year in Korea during the Spring Season (KMA, 2001). The occurrence days and intensity of YS recently tend to increase a little in 2000 and 2001 (Table 1). Recently, it appears to be a little increase in the occurrence days and intensity. In addition, it is not restricted to the springtime period only. The remarkably distinctive YS episode was observed during 25-27 January 1999.

The objective of this study is to explore transport and chemical characteristics of Yellow Sand in Korea. General characteristics of dust and its relationship with $O_3$ are briefly described during the observed distinctive YS events in 1999 and 2000. A special emphasis would be put on the episodic case of January 1999 through the observational analysis and simplified modeling.

Table 1. Frequencies and occurrence days of YS in Korea during 1990 – 2001.

| | 1990 | 1991 | 1992 | 1993 | 1994 | 1995 | 1996 | 1997 | 1998 | 1999 | 2000 | 2001 |
|---|---|---|---|---|---|---|---|---|---|---|---|---|
| Frequency | 1 | 4 | 3 | 5 | 0 | 5 | 1 | 1 | 3 | 3 | 6 | 4 |
| Occurrence days | 3 | 11 | 8 | 14 | 0 | 13 | 1 | 1 | 13 | 6 | 10 | 18 |

## 2. METHODOLOGY

### 2.1. Observation Method

The remarkably distinctive episodes are selected for the general description of YS. They are briefly explained in Table 2. Additionally, four sites (Kangwha, Seoul, Wonju, and Ulleng) of the routine air pollution-monitoring network of Korea were chosen for the analysis (Fig. 1). Monitoring locations were chosen to the direction of the dust storm propagation. The measured compounds included $O_3$, and particle matter (PM10) whose diameter is less than 10 μm. Ozone was measured with Dasibi (1008 AH) by UV photometric method, and PM10 with Dasibi (7001) by β -ray absorption method. Detection limits and measuring ranges for $O_3$ are 1.0ppb and 1 ~ 1000ppb while those of TSP are 2 $\mu g\ m^{-3}$ and 2 ~ 1000 $\mu g\ m^{-3}$, respectively. A cascade impactor (Anderson, AN-200) was used to identify the particle size distribution of aerosol at the Bulkwang monitoring site in Seoul for January YS 1999. The sampling was carried out from 1500 LST 25 January to 1215 LST 27 January 1999 for the YS event and 1040 LST 28 January to 1020 LST 1 February 1999 after the YS period (AYS).

Table 2. Brief descriptions of the chosen YS episodes.

| Given name | Period | Max. PM10 Concentration ($\mu g\ m^{-3}$) | Dust plume type and shape | Persistence |
|---|---|---|---|---|
| JS_YS | 25-27 Jan. 1999 | 908 (Seoul) [1)] | Distinctive bimodal shape with strong and wide spread plumes | Almost 3 days |
| MS_YS | 23-24 Mar. 2000 | 941 (Ulleng) | Bimodal shape in strong intensity | About 1 day |
| MW_YS | 27-28 Mar. 2000 | 233 (Ulleng) | Bimodal shape in weak intensity | About 2 days |
| AS_YS | 7-8 Apr. 2000 | 822 (Wonju) | Unimodal with a sharp dust pulse | Half a day |

[1)] Parenthesis represents the site where the maximum hourly concentration of PM was observed.

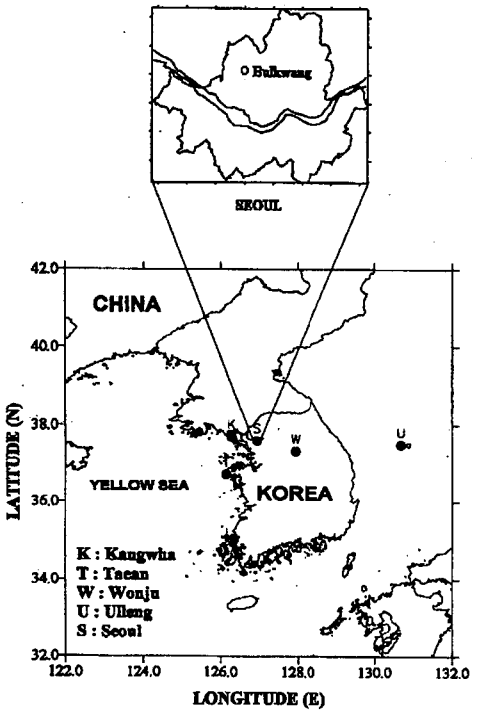


Fig.1. Analysis domain and locations of monitoring sites in Korea. K : Kangwha, S : Seoul, W : Wonju, U : Ulleng, and T : Taean.

Analyzed species of both samples were ion components such as $SO_4^{2-}$, $NO_3^-$, $Cl^-$, $NH_4^+$, $K^+$, $Ca^{2+}$, $Na^+$, and $Mg^{2+}$. Water-soluble species were extracted with 20 ml of distilled and deionized water for 60 min. Concentrations of $SO_4^{2-}$, $NO_3^-$, and $Cl^-$ were determined by the ion chromatography (Dionex-500). Concentrations of $K^+$, $Ca^{2+}$, $Na^+$, and $Mg^{2+}$ were analyzed by the atomic absorption spectroscopy (Varian, SpectraAA 800), while that of $NH_4^+$ was determined by indophenol colorimetric method (Perkin-Elmer, Lambda 20).

### 2.2. Lagrangian Approach

YS plumes are found to propagate as episodic dust pulses according to the temporal variation of dust concentration (Kim and Park, 2001). Substantial variability is indicated on time scales. During the YS event, dust concentrations occasionally exceed the background levels by up to 2-3 orders of magnitude. Therefore, a conceptual Lagrangian-type approach could be introduced in this study. The variation in concentration of sulfur species along the trajectory can be described as (Klaic, 1996),

$$\frac{Ds_1}{Dt} = -\left(\frac{V_{d1}}{h} + k_p\right)s_1 + f\frac{Q}{h} \quad (1)$$

$$\frac{Ds_2}{Dt} = -\frac{V_{d2}}{h}s_2 + \frac{3}{2}k_p s_1 \quad (2)$$

where D/Dt is the total Lagrangian time derivative, $s_1$ and $s_2$ are concentrations of $SO_2$ ($\mu g\ m^{-3}$) and $SO_4^{2-}$ ($\mu g\ m^{-3}$) in air, $v_{d1}$ and $v_{d2}$ are dry deposition velocities ($m\ s^{-1}$) of $SO_2$ and $SO_4^{2-}$, respectively, h is the mixed layer height (m), Q is the sulfur emission per unit area and time ($\mu g\ m^{-2}\ s^{-1}$), and $k_p$ is the transformation rate of $SO_2$ to $SO_4^{2-}$ ($s^{-1}$). $f$ denotes the part of sulfur emission emitted in the form of $SO_2$.

Because biogenic sulfur emission is very small compared to anthropogenic sulfur emission over the Yellow Sea, we could neglect the emission term over the Yellow Sea. Arimoto et al. (1996) showed that biogenic emissions including DMS and MSA over the Yellow Sea could be neglected in comparison to anthropogenic sulfur compounds. According to the KIST survey (1998), MSA/nss-$SO_4^{2-}$ ratio was about 0.4~5.4%, indicating clearly low level of MSA compared to another background region. They suggested that it might be attributed mainly to the dominant effect of anthropogenic $SO_2$ conversion to sulfate in Northeast Asia.

### 2.3. Chemical Mechanism

It is hypothesized that reactions of $SO_2$ on the dust surface are important pathway for the production of particulate sulfate for the high dust loading such as Yellow Sand. The air parcels consist of long-range transported dust particles. It is also assumed that particles are initially dry, spherical, neutral in charge, and internally well mixed. Of course, dust particles are originally never spherical, however, they get curved during the transport. In this study, we are not looking into source region in detail, but the downwind region is, to some extent, far away from the source region.

All particles at a given size have the same composition. The dust particles are assumed to be a lognormal size distribution. A typical observed size distribution of YS at Seoul ranges 0.1 to 20$\mu m$. The size, density, and mass distributions of the dust particles used in this study are given in Table 3.

Table 3. Physical properties of dust particles used in the study.

| Number of particle (bin) | Bin 1 | Bin 2 | Bin 3 | Bin 4 | Bin 5 |
|---|---|---|---|---|---|
| Size range (㎛) | 0.1- 0.5 | 0.5-1.5 | 1.5-6.0 | 6.0-10.0 | 10.0-20.0 |
| Mean diameter (㎛) | 0.38 | 1.0 | 3.5 | 8.0 | 15.0 |
| Mean density (g $cm^{-3}$) | 2.5 | 2.5 | 2.5 | 2.5 | 2.5 |
| % of total number | 18.2 | 64.6 | 17.0 | 0.30 | 0.00 |
| % of total mass | 0.14 | 12.8 | 63.7 | 19.8 | 3.5 |

The number distribution can be given as

$$\frac{dN}{d\log r} = \frac{n}{\sqrt{2\pi}\log\sigma}\exp\left\{\frac{-(\log r/R)^2}{2(\log\sigma)^2}\right\} \quad (3)$$

where n, r, R and σ are the number concentration, the particle radius, the number mean radius and the standard deviation, respectively. An average density of the dust particle is assumed to be 2.5 g $cm^{-3}$ (Arao and Ishizaka, 1986).

The formation of secondary sulfate aerosol is modeled using the semi-empirical equation for binary homogeneous nucleation of $H_2SO_4$ and $H_2O$ introduced by Peter and Easter (1992).

$$J_n = r_1(S_s)^{r_2} \quad (4)$$

where $J_n$ is the homogeneous nucleation rate ($cm^{-3}$ $sec^{-1}$), and $S_s$ is the saturation ratio of the sulfuric acid vapor, which is defined as the ratio of the actual vapor pressure of $H_2SO_4$ to its saturation vapor and $r_1$ and $r_2$ are empirical parameters which depend on relative humidity (RH).

The absorption of $SO_2$ and subsequent conversion to nss-sulfate by dissolved oxidants such as $H_2O_2$, OH, and $O_3$ on given particle size modes (Zhang and Carmichael, 1999) may be parameterized by

$$SO_2 + O_x + X(i) \xrightarrow{H_2O} XSO_4(i) \quad (5)$$

where $O_x$ represents the dissolved oxidants such as $O_3$, OH, and $H_2O_2$. X(i) the i-th aerosol size bin, and $XSO_4$(i) the corresponding sulfate aerosol within the same size bin.

If the mass transport coefficient, $k_p$ of the above reaction (Eq. 5) follows a pseudo-first order reaction (Heikes and Thompson, 1983; Fuchs and Sutugin, 1970), then

$$k_p = \int_{r1}^{r2} k_d \frac{dn}{dr} dr \quad (6)$$

$$k_d = \frac{4\pi r D_j}{1 + f(K_n,\alpha)K_n} \quad (7)$$

$$f(K_n,\alpha) = \frac{1.333 + 0.71K_n^{-1}}{1 + K_n^{-1}} + \frac{4(1-\alpha)}{3\alpha} \quad (8)$$

where Kn is the Knudsen number, defined as th ratio of the effective mean free path of a gas molecule in air, λ , to the particle radius r, $k_d$ the size dependent mass transfer coefficient [$cm^3s^{-1}$], D [$cm^2s^{-1}$] the molecular diffusion coefficient in air, dn/dr the number size distribution of aerosol particles, and α the dimensionless mass accommodation coefficient.

## 3. RESULTS AND DISCUSSION

### 3.1. Observational Feature

#### 3.1.1. General Characteristics of Yellow Sand

PM10 for the wintertime YS of 1999 and springtime YS of 2000 are summarized in this section. Four-day hourly data of each episode are equivalently analyzed. Table 4 shows the percentile values of the distinctive episodes of 1999 and 2000 YS phenomenon together with those of spring non-YS period of 2000. Percentiles more than 50% values only are given since there is no significant difference in percentiles less than 50%. The starting time of the YS event in Korea is assumed to be the time when hourly average concentration of PM10 exceeded 150 μg $m^{-3}$, which is the national short-term criteria for the hourly average concentration.

The median values are 108.5, 54.5, 71.0, and 90.5 μg $m^{-3}$ for JS_YS, MS_YS, MW_YS, and AS_YS, respectively, while the maximum values are 908.0, 696.0, 225.0, 750.0 μg $m^{-3}$ for each episode in Seoul (Table 4). Fig. 2 shows the percentile concentrations of PM10 for each YS episode and those of spring non-YS period of 2000. From 80 percentiles of mass concentrations are sharply increased especially in the March strong YS (MS_YS) and April Strong YS (AS_WS). However, March YS with weak intensity (MW_YS) has very similar distribution of mass concentrations to those of non-YS in spring of 2000 (A_NYS). It should be substantial increases in mass concentration compared to the non-YS period. The annual average concentration of PM10 for all stations in Korea is 70 μg $m^{-3}$ (MOE, 1999). It is found out that maximum concentrations of the different locations for the same dust plume showed 10-30% variation, therefore aerosol mass loadings could change a lot within a few of hundred km (Table 4).

Ratios of median and 100% percentile differences of each episode (JS_YS, MS_YS, MW_YS, and AS_YS) to those of A_NYS are 5.3, 5.5, 0.9, and 4.8, respectively. Those values of strong YS events are shown to be about 5 times higher than those of weak YS.

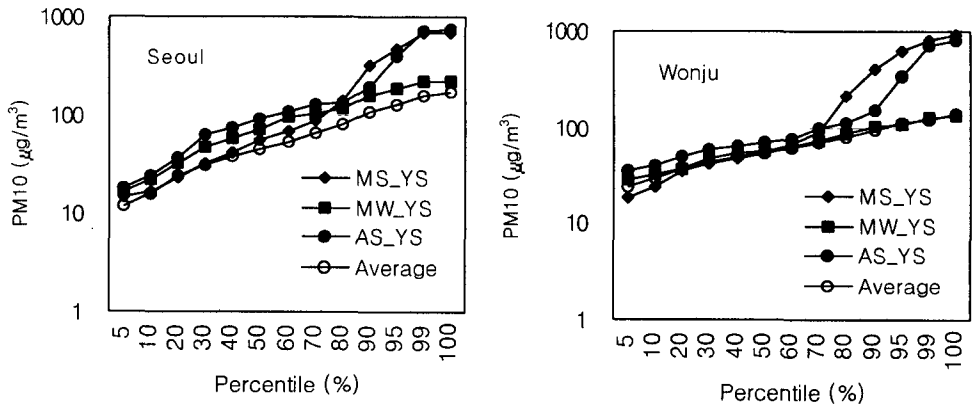


Fig. 2. Percentile distributions of PM10 for each YS episode and those of spring NYS period .

Table 4. Percentile summary of PM10 for each YS episode and non-YS period of 2000 at Kangwha, Seoul, Wonju and Ulleng island (unit : μg $m^{-3}$).

| Period * | Percentile | Kangwha | Seoul | Wonju | Ulleng | Average |
|---|---|---|---|---|---|---|
| 25-28 Jan 1999 | 50 | 105 | 108.5 | 97.5 | 118 | 107.3 |
| (JS_YS) | 60 | 217 | 170 | 138 | 164 | 172.3 |
| | 70 | 366 | 272.5 | 225 | 225 | 272.1 |
| | 80 | 519 | 394 | 279 | 393 | 396.3 |
| | 90 | 670 | 463 | 321 | 529 | 495.8 |
| | 95 | 713 | 501 | 348 | 631 | 548.3 |
| | 99 | 796 | 753.2 | 691 | 888 | 782.1 |
| | 100 | 826 | 908 | 730 | 893 | 839.3 |
| 23-26 Mar 2000 | 50 | 56.0 | 54.5 | 55.0 | 61.0 | 56.6 |
| (MS_YS) | 60 | 63.0 | 70.0 | 67.0 | 75.0 | 68.8 |
| | 70 | 78.0 | 88.5 | 90.0 | 85.5 | 85.5 |
| | 80 | 153.0 | 141.0 | 209.0 | 215.0 | 179.5 |
| | 90 | 345.0 | 329.0 | 413.5 | 407.0 | 373.6 |
| | 95 | 440.5 | 473.3 | 625.8 | 520.3 | 515.0 |
| | 99 | 590.8 | 675.1 | 811.9 | 817.5 | 723.8 |
| | 100 | 624.0 | 696.0 | 904.0 | 941.0 | 791.3 |
| 26-29 Mar 2000 | 50 | 67.5 | 71 | 57.5 | 58.5 | 63.6 |
| (MW_YS) | 60 | 81 | 96 | 64 | 64 | 76.3 |
| | 70 | 100.5 | 104 | 74.5 | 68.5 | 86.9 |
| | 80 | 123 | 119 | 88 | 81 | 102.8 |
| | 90 | 144.5 | 159.5 | 104.5 | 148 | 139.1 |
| | 95 | 166 | 184.8 | 108 | 162.8 | 155.4 |
| | 99 | 188.7 | 219.3 | 129.3 | 226.4 | 190.9 |
| | 100 | 221 | 225 | 135 | 233 | 203.5 |
| 6-9 Apr 2000 | 50 | 103 | 90.5 | 70.5 | 81 | 86.3 |
| (AS_YS) | 60 | 138.8 | 107 | 77 | 97 | 105.0 |
| | 70 | 157.5 | 126.5 | 98 | 109 | 122.8 |
| | 80 | 182 | 136 | 110 | 139 | 141.8 |
| | 90 | 271 | 192 | 151.5 | 194 | 202.1 |
| | 95 | 307.7 | 392.8 | 344.5 | 225.8 | 317.7 |
| | 99 | 719.4 | 714.9 | 705.2 | 392 | 632.9 |
| | 100 | 720 | 750 | 822 | 392 | 671.0 |
| Average of non-YS | 50 | 48 | 45 | 55 | 57 | 51.3 |
| 2000 | 60 | 54 | 54 | 62 | 64 | 58.5 |
| (A_NYS) | 70 | 61 | 65 | 70 | 77 | 68.3 |
| | 80 | 73 | 80 | 79 | 97 | 82.3 |
| | 90 | 94 | 108 | 94.3 | 132 | 107.1 |
| | 95 | 129 | 131 | 111 | 165 | 134.0 |
| | 99 | 169 | 158 | 124 | 206 | 164.3 |
| | 100 | 202 | 175 | 139 | 342 | 214.5 |

* 4-day data are used for each YS period, whereas 50-day data for non-YS period

### 3.1.2. $O_3$ and Dust Interaction

Temporal variations of particle matter, $O_3$, relative humidity and insolation are investigated to understand the relationship between $O_3$ and dust. March Strong YS (MS_YS) from 22 to 25 March, was observed from late afternoon to midnight. Hourly maximum concentration of PM10 reached to about 700 μg $m^{-3}$, while $O_3$ remarkably decreased at once. Relative humidity ranged from 40 to 60% during the YS period. Relative humidity was not low during the YS event including the others. As explained later, it could be a favorable condition for the absorption and subsequent conversion of $SO_2$ and NOx into sulfate and nitrate. Interestingly, first plume of MS_YS passed over Ulleng island at midnight, and then $O_3$ clearly showed anti-correlation with PM10 (Fig. 3a). The decrease in $O_3$ concentration during the YS event could be attributed to several pathways. For instance, the direct uptake of $O_3$ or the destruction of important precursors on the wetted dust surface can cause $O_3$ decrease. The next possible pathway will be the direct reduction in photolytic rates inducing a decrease in $O_3$ formation rates. However, it was nighttime when the dust plume passed over Ulleng island, so the latter contribution to $O_3$ formation will be not important. It clearly shows

the distinctive evidence for significant loss of $O_3$ during the YS period, and direct uptake of $O_3$ on the dust surface during the nighttime.

The next episode of March Weak YS (MW_YS) from 26 to 29 March had somewhat different characteristics especially in intensity and PM10 and $O_3$ relationship, compared to the others. Above all, PM10 and $O_3$ concentrations showed similar time variations. Since YS arrived at the Korean peninsula during the daytime, it is difficult to estimate dust effect on $O_3$ variation. $O_3$ concentrations were well correlated with PM10 concentrations (r=0.84) especially in Ulleng (Fig. 3b). It could imply the dust transport together with $O_3$ during the weak YS period.

In 6 to 9 April of Strong YS (AS_YS), mass concentration of PM10 increased during the daytime. YS phenomenon was detected from 1100LST to 1800LST on 7 April with the maximum value of 750 $\mu g\ m^{-3}$ in Seoul. $O_3$ remarkably decreased during the daytime in contrast to the increase in PM10 concentration (Table 5). Direct inference of $O_3$ chemical loss from observations is difficult because of the long lifetime of Ox (Jacob, 2000). However, a global 3-D model study by Dentener et al. (1996) investigated the potential effects of uptake of $O_3$ by mineral dust. Results showed a 10% decrease of boundary layer $O_3$ in dusty regions, mostly because of direct uptake of $O_3$ by dust, while outside dusty regions the effect was negligibly small. Insolation and $O_3$ together decreased by 10% and 20%, respectively, whereas PM10 remarkably increased by a factor of 7-10. Both of them also decreased by about 30% relative to the increase of PM10 more than 10 times larger than the former day in Wonju (Table 5). It is difficult to identify how much the direct uptake of $O_3$ or relevant precursors and the reduction of insolation could contribute in the $O_3$ decrease.

Table 5. Maximum values of insolation, O3, and PM10 at Seoul and Wonju during the AS_YS period.

| Site | Maximum value of | Date | | | |
|---|---|---|---|---|---|
| | | 6 April | **7 April (YS event)** | 8 April | 9 April |
| Seoul | Insolation ($MJ\ m^{-2}$) | 2.68 | **2.37** | 2.58 | 1.72 |
| | $O_3$ (ppb) | 51 | **41** | 54 | 48 |
| | PM10 ($\mu g\ m^{-3}$) | 107 | **750** | 188 | 162 |
| Wonju | Insolation ($MJ\ m^{-2}$) | 3.27 | **2.40** | 3.28 | 2.05 |
| | $O_3$ (ppb) | 49 | **36** | 45 | 48 |
| | PM10 ($\mu g\ m^{-3}$) | 76 | **822** | 154 | 122 |

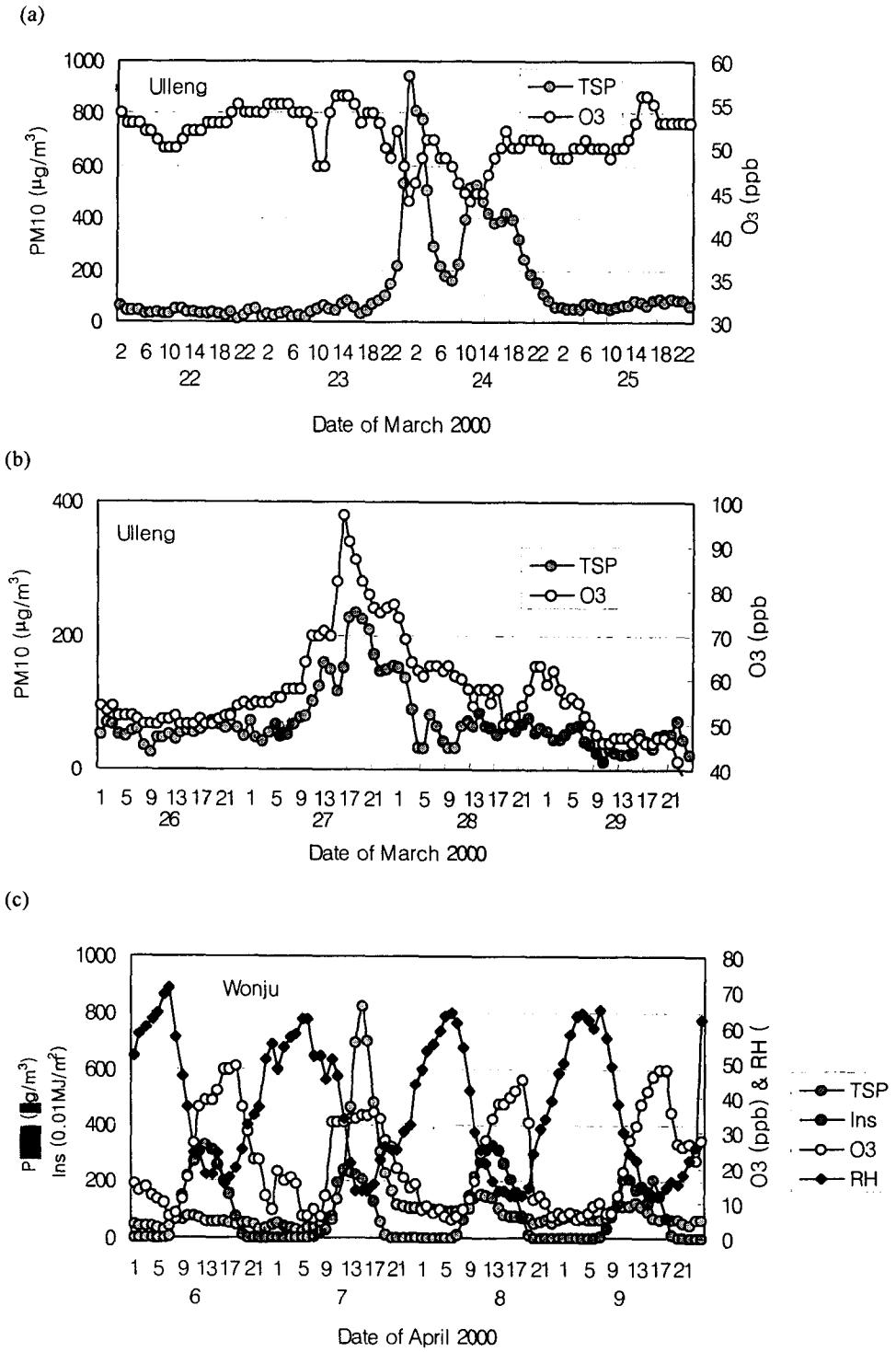


Fig. 3. PM and $O_3$ relationship for the episode of MS_YS (a) and MW_YS(b) at Ulleng island together with PM, $O_3$, insolation, and relative humidity for AS_YS episode at Wonju (c).

### 3.1.3. Particle Size Distribution of YS

Particle size distributions obtained from the cascade impactor were shown in Fig. 4 for the YS and AYS periods. This comparison made it possible to investigate how the size distribution of dust particles could change under the different dust loadings. The dominant ion components were $SO_4^{2-}$, $NO_3^-$, $Ca^{2+}$ and $Na^+$ with the total sum of 8-stage cascade impactor filter concentrations of 11.3, 7.6, 6.1 and 4.2 $\mu g\ m^{-3}$ respectively, compared to the corresponding concentrations of 4.1, 4.6, 0.4, and 1.2 $\mu g\ m^{-3}$ after the passage of YS over Korea (Fig. 4). Most ion components increased for all sizes during the YS period, compared to the AYS period. Concentrations of $SO_4^{2-}$, $Ca^{2+}$ and $Mg^{2+}$ during the YS period were ten times larger than those in the AYS period especially in the size of 3.3~4.7$\mu m$. The mode diameter of these compounds for the YS event was around 4$\mu m$, compared to 0.4~0.9$\mu m$ of AYS, indicating a significant amount of $SO_4^{2-}$ and $NO_3^-$ formations on the coarse mode during the long-range transport of Yellow Sand. However, the maximum concentration of $NH_4^+$ was found in the fine particle of diameter less than 2$\mu m$ for both YS and AYS samples. These observational findings are quite consistent with the measurement results by Nishikawa et al (1991) at Yaku Island during the Yellow sand event except for the sulfate distribution. The size-resolved composition showed a main peak of sulfate in the coarse mode in this study, whereas there were bi-modal peaks, one of which was in the fine mode, and the other in the coarse mode at Yaku Island.

The sulfate distribution on dusty days showed a large fraction of sulfate in the coarse mode also in the report of Parungo et al (1996). The coarse mode has more sulfate concentration than the fine mode due to the larger available surface area in the coarse mode, and most of the calcium cations exist in the coarse mode. The sulfate distribution in Seoul Korea during this YS event was similar to that near source region in Beijing (Parungo et al., 1996) rather than at Yaku island (Nishikawa et al., 1991).

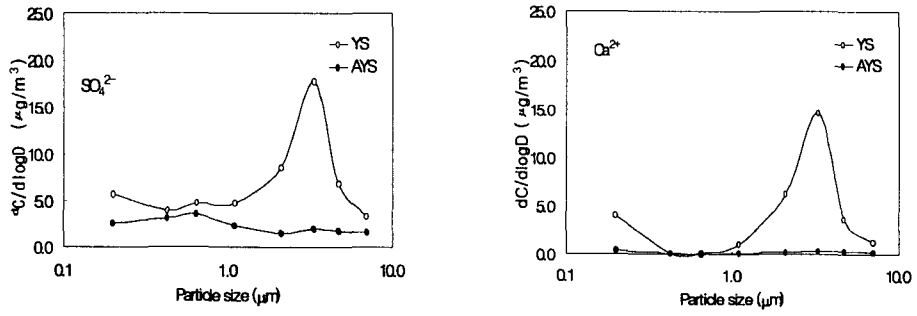


Fig. 4. Particle size distributions of the major ion components ($SO_4^{2-}$ and $Ca^{2+}$) during the Yellow Sand event (25~27 January) and after the YS period(28 January~1 February).

The analysis of the equivalent molar ratio for the anion and cation showed that $SO_4^{2-}$ and $NO_3^-$ concentrations were well correlated with $NH_4^+$ during the AYS period, whereas they were equivalently balanced with $Ca^{2+}$ during the YS event. It suggests that the compounds of YS aerosols were in the form of $CaSO_4$ and $Ca(NO_3)_2$. The equivalent molar ratio of nss-$Ca^{2+}$/$Na^+$ remarkably increased to 1.5~2.3 especially in the range of 2.1 to 7.0$\mu m$ of particle diameter for the YS event, but less than 0.5 for the AYS period. The increase in the ratio was due to mainly an increase in nss-$Ca^{2+}$.

## 2.1. Model Results

### 3.2.1. Assumptions and Initializations

The observed lognormal size distribution at Seoul was selected for the model analysis during a winter-time Yellow Sand event occurred on 25~28 January 1999. Observed average mass concentration was about 300 $\mu g\ m^{-3}$, and the number mean radius, r is 0.88 $\mu m$ with standard deviation of log $\sigma$ of 0.3. The calculation of dry deposition velocity for gases is estimated by the aerodynamic resistance, the quasi-laminar sublayer resistance, and the surface resistance or canopy resistance (Wesley and Hicks, 1977). In this study, dry deposition velocities of $SO_2$ and $SO_4^{2-}$ are assumed to be $8\times 10^{-3}$ m $s^{-1}$ and $1\times 10^{-3}$ m $s^{-1}$ over

the Yellow Sea (Berge and Jakobsen, 1998). While the air parcel moves through the Yellow Sea, constant values of dry deposition velocity of $SO_2$ and $SO_4^{2-}$ ($V_{d1}$ and $V_{d2}$) are applied.

This study domain includes pathway of Yellow Sand just staring at the NEC (Northeast region of China), through the Yellow Sea, and arriving at WEK (Western region of Korea) as previously emphasized. Dust laden air masses move from NEC through the Yellow Sea to WEK for approximately 12 hours based on the estimated propagation speed of Yellow Sand of 70 km $hr^{-1}$ (Kim and Park, 2001). Chung (1996) suggested that Korea experiences two types of YS events. One is mainly confined in the elevated mixed layer so that the ground-level concentration is low. This could be transported to the north Pacific or even up to North America. The other is transported in the lower boundary layer along the terrain, thus inducing high ground-level concentrations in Korea. Actually, Murayama et al. (1998) observed some dust layers in the middle troposphere which could not much intrude into the boundary layer in Japan. We are interested in the latter one since it directly affects air quality in Korea. It is also assumed that no mass transport takes place through the top of the mixed layer whose average height is assumed to be 1500 m. Air pollutants are assumed to be well mixed in the mixed layer around the Yellow Sea based on aircraft measurements for the years from 1998 to 1999 (Kim et al., 2001). Based on the observation of a Yellow Sand event on 25~27 January 1999, temperature and relative humidity are assumed to be 280K (275 ~285K) and 60% (50~70%), respectively (KMA, 1999). The dust loading in the domain ranges 100~300 $\mu g$ $m^{-3}$ during the dust storm period.

It is assumed that absorption and heterogeneous reactions of the modeled species on the dust surface are irreversible and the reaction of $SO_2$ is limited by the gas-phase diffusion. These assumptions can be justified for most condensing species considered in this work when dust particles contain some water, which is the most likely case as observed by Hanel (1976). In addition, the absolute amounts of alkaline mineral dust during the YS period are large enough to support sulfate formation on the aerosol surface.

One of the important parameters critically relating to sulfate formation on the aerosol surface is relative humidity (RH). Let us briefly examine RH during the wintertime YS event when a significant amount of sulfate and nitrate were formed in Korea. Wintertime YS event was observed on 25-27 January 1999 in Korea. RH was unexpectedly not low during the event with the diurnal mean relative humidity of 57-66%, and temperature was 3.8-5.0°C at Seoul (KMA, 1999). These values were a little higher than the monthly averages of January (58% and –0.8 °C). These conditions could facilitate the possibility of sulfate formation on the mineral aerosol over the Yellow Sea. Dust could be coated by an aqueous film through the condensation of water vapor at relative humidity higher than 50% as was the case in the present YS event. Dust coated with an aqueous film can provide a site for the heterogeneous reactions for the conversion of absorbed $SO_2$ and NOx to sulfate and nitrate.

### 3.2.2. Mass Accommodation Coefficient

The mass transport coefficient ($k_p$) highly depends on the mass accommodation coefficient ($\alpha$ ). $k_p$ increases with the increase of $\alpha$ and reaches a maximum when $\alpha$ is around 0.1. However, as the mass accommodation coefficient highly depends on colliding species and the state of aerosol surface states, the estimation of $\alpha$ value is highly uncertain.

The mass accommodation coefficients of hygroscopic inorganic gaseous species such as $HNO_3$, $NH_3$, $H_2SO_4$, and HCl on water droplets are considered on the order of 0.1 (Worsnop et al., 1989; Dentener, 1993), but Wexler et al. (1994) suggested $\alpha$ =0.01 for the hygroscopic species. These species are directly sorbed onto or desorbed out of the aerosol surfaces. However, the $SO_2$ uptake is more complicate because the irreversible sorption of $SO_2$ is subsequently followed by several aqueous reactions (Maahs, 1983; Dentener et al., 1996). The measured $\alpha$ for $SO_2$ at 260-292K on liquid water surfaces is about 0.11 (Worsnop et al., 1989), while it is 0.3× $10^{-3}$ at room temperature on the surface of amorous carbon (Rogaski et al., 1997). Dentener et al. (1996) pointed out that the oxidation of $SO_2$ by $O_3$ in the aqueous phase is very fast in the presence of water and thus oxidation reaction facilitates the $SO_2$ mass transport. Most recently, Song (1999) utilized $\alpha$ ($SO_2$)=0.05 and 0.005 at different humidity conditions. Based on previous studies, the values of $\alpha$ ($SO_2$) are selected from 0.001 to 0.1 with a reference value of 0.005 in this study.

$k_d$ (the diffusion rate constant) and $k_p$ (the mass transport coefficient) are important factors in determining the magnitude of heterogeneous surface uptake. They are highly dependent on the particle size for different species (Fig. 5). The values of $k_d$ increase linearly with particle size with the order of $10^{-7}$ ~ $10^{-4}$ $cm^3 s^{-1}$. The values of $k_p$ are determined by the values of $k_d$ and the number concentration as in equation (8). The values of $k_p$ are on the order of $10^{-7}$ ~ $10^{-5}$ $s^{-1}$ with the maximum values in the diameter range of 1.5~6.0 $\mu m$. The distribution of $k_p$ is closely related with the log normal distribution of the particle number concentration.

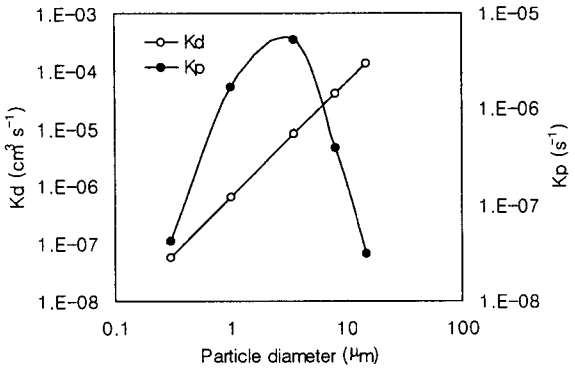


Fig. 5. The diffusion rate coefficient and the mass transport coefficient of $SO_2$ as a function of particle size.

### 3.2.3. The Relative Importance of Conversion to Deposition

Fig. 6a shows temporal variations of the $SO_2$ and $SO_4^{2-}$ concentrations at various mass accommodation coefficients from 0.001 to 0.05 for the 1/2-day period through the heterogeneous reaction process only. Generally $SO_4^{2-}$ is steadily produced with the depletion of $SO_2$. The results show a remarkable increase in sulfate formation with the increase in α value. The increase in sulfate concentration continues until $SO_2$ being completely depleted. As a result, the sulfate formation strongly depends on the $SO_2$ concentration.

Fig. 6b represents the variations of $SO_2$ and $SO_4^{2-}$ concentrations at various mass accommodation coefficients for the 1/2-day period including the deposition process. The overall trend is the same as in the heterogeneous reaction only in Fig. 6a. However, the $SO_4^{2-}$ concentration significantly decreases compared to that of the heterogeneous case only due to dry deposition added. The decreasing rate of $SO_4^{2-}$ concentration strongly depends on the mass accommodation coefficient.

(a) (b)

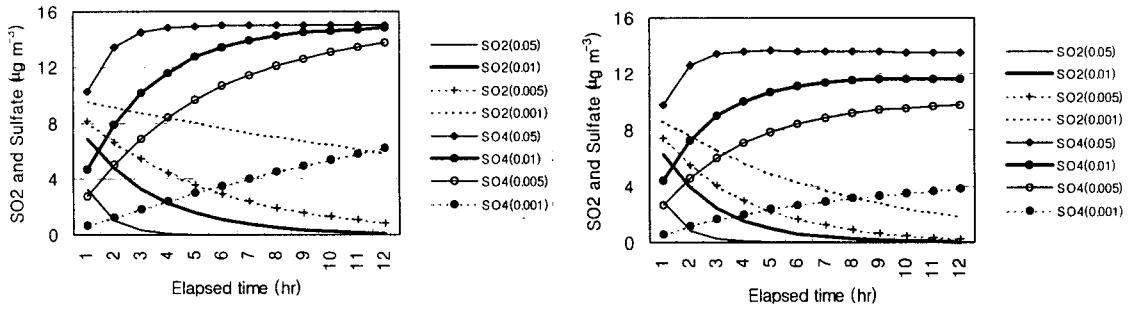


Fig. 6. Formation of particulate sulfate and reduction of $SO_2$ through (a) the heterogeneous reaction and (b) the heterogeneous reaction with deposition process for various mass accommodation coefficients. The number in the parenthesis denotes the mass accommodation coefficient.

The ratio of the heterogeneous conversion rate (second term in Eq. (1)) to dry deposition process (first term in Eq (1)) is defined as the 'Conversion To Deposition ratio (COD)'

$$COD = \frac{k_p h}{V_{d1}} \tag{9}$$

If COD is larger than 1, the transformation is more predominant than the deposition process. If the $SO_2$ dry deposition velocity is to be 0.8 cm s$^{-1}$ over the sea, COD becomes unity when α is $6.0\times 10^{-4}$ for this case. This ratio is similar to sulfate yield, fraction of $SO_2$ oxidized to sulfate in the atmosphere.

Table 6 shows comparisons of the simulation results with or without deposition processes. COD ratio is also included in Table 6. The effect of the heterogeneous reaction is predominant when $\alpha > 6\times 10^{-4}$, whereas the deposition effect becomes important when $\alpha < 6\times 10^{-4}$. Therefore, the conversion process is

more important than the deposition process for the formation of $SO_4^{2-}$ for the given YS condition.

The heterogeneous conversion rates of $SO_2$ to sulfate are 3.2, 14.4, 25.8, and 70.9% $hr^{-1}$ at $\alpha$ =0.001, 0.005, 0.01, and 0.05, respectively. These values are 1.5 ~ 100 times greater than homogeneous oxidation rates of 0.5 ~ 2% $hr^{-1}$ (Wexler et al., 1994), and comparable to and also greater than 6 ~ 8% $hr^{-1}$ in the plume of Kuwait oil fires (Herring er al., 1996). These high conversion rates can also be analyzed in comparisons of aerosol surface area to the underlying ground surface. The total surface area of aerosols is assumed to be 1.52× $10^{-6}$ $cm^2$ $cm^{-3}$ and vertically well mixed within the 1.5-km layer. Then the aerosol surface available for reactions could be more than 23% of the ground surface. In addition, the deposition process occurs only in the bottom layer of air, whereas the heterogeneous conversion process occurs in the whole mixed layer. The reaction of $SO_2$ with dust is so fast that a significant amount of $SO_2$ can be converted to sulfate during the transport of Yellow Sand.

Table 6. Comparisons of sulfate formation with or without deposition process after a 12-hr simulation.

| α | Only chemistry | | Chemistry with deposition | | Mass transport coefficient ($s^{-1}$) | COD[1)] | Turnover time (hr) |
|---|---|---|---|---|---|---|---|
| | $SO_2$ ($\mu g\ m^{-3}$) | $SO_4^{2-}$ ($\mu g\ m^{-3}$) | $SO_2$ ($\mu g\ m^{-3}$) | $SO_4^{2-}$ ($\mu g\ m^{-3}$) | | | |
| 0.001 | 4.09 | 8.86 | 0.30 | 4.4 | 8.80× $10^{-6}$ | 2.6 | 20 |
| 0.005 | 0.17 | 14.8 | 0.01 | 10.0 | 4.00× $10^{-5}$ | 12.0 | 6 |
| 0.01 | 0.01 | 15.0 | 0.00 | 11.4 | 7.18× $10^{-5}$ | 21.5 | 4 |
| 0.05 | 0.00 | 15.0 | 0.00 | 13.1 | 1.97× $10^{-4}$ | 59.1 | 1.5 |

[1)] COD = Mass transport coefficient / dry deposition ratio

We can obtain the turnover time (mean residence time: $\tau$) of $SO_2$ by taking the reciprocal of the mass transfer coefficient and deposition rate. The result of this study shows that $\tau$ varies from 1.5 to 20 hrs for the mass accommodation coefficient from 0.001 to 0.05. $SO_2$ turnover times from the present results are quite smaller than previous investigations (Benkovitz et al., 1994) due to the heterogeneous conversion.

### 3.2.4. Comparisons with Observation

In addition to the ambient precursor concentrations and mass accommodation coefficients, sulfate formation also strongly depends on the particle size. Fig. 7 shows the comparison of calculated size distribution at the dust loading of 300 $\mu g\ m^{-3}$ with the observation. In this case, the total sulfate formation is about 10 $\mu g\ m^{-3}$. The difference of the sulfate concentration in fine mode is relatively large. However, most sulfate is formed on the dust surface in the size range of 1.5 ~ 6.0 $\mu m$. These sulfate distributions are quite consistent with the observation results for a wintertime Yellow Sand event (Kim and Park, 2001). This is due to the fact that the formations of sulfate is mainly determined by the mass transport coefficient, which is the highest in the size of 1.5 ~ 6.0 $\mu m$. As $SO_2$ is oxidized to $H_2SO_4$, the $H_2SO_4$ may undergo heteromolecular nucleation with $H_2O$ to form new sulfate particles or may deposit on the pre-existing particles through condensation and absorption processes. The new sulfate particle produced by nucleation can further grow and form larger particles through coagulating one another and/or with pre-existing particles. At a lower dust loading, the absorption rate is relatively small, and sulfate formation occurs in the fine mode (0.1 ~ 1.0 $\mu m$, accumulation mode) through the nucleation and coagulation processes. Generally, the $SO_2$ and $H_2SO_4$ irreversibly condense onto both fine and coarse modes. Since the fine-mode mass transport coefficient is generally larger than the coarse-mode coefficient, sulfate preferably forms in the fine mode. However, the sulfate formation due to surface deposition predominates for dust loading of more than 100 $\mu g\ m^{-3}$ because of a large number density of pre-existing dust and a larger absorption rate of $SO_2$.

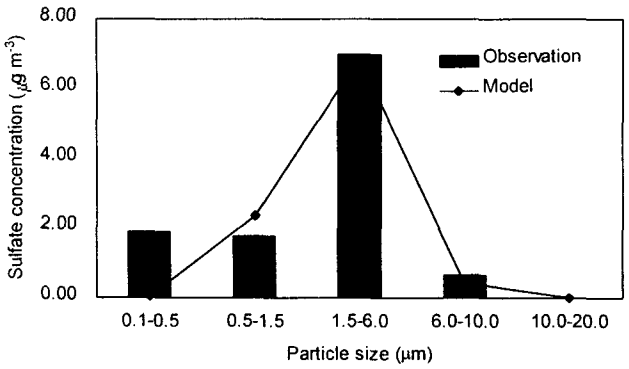


Fig. 7. The estimated and observed sulfate distributions for a dust loading of 300 μg $m^{-3}$.

## 3. CONCLUSIONS AND RECOMMENDATIONS

The physical and chemical properties of Yellow Sand events observed observed in Korea in 1999 and 2000 were investigated. Additionally, transport and transformation of sulfur compounds over the Yellow Sea were examined with the conceptual Lagrangian-type gas-aerosol model.

The selected YS phenomena were remarkably distinctive episodes in the occurrence time and intensity that had ever been observed in Korea. During the episode period, aerosol mass loadings changed by an order of magnitude within a few hours and a few of hundred km. $O_3$ had a anti-correlation with PM10 during the strong YS events, while $O_3$ was rather well correlated with PM10 during the weak YS event. Results show the distinctive evidence for significant loss of $O_3$ during the YS period, and the remarkable direct uptake of $O_3$ on the dust surface during the nighttime.

$SO_4^{2-}$, $NO_3^-$, $Ca^{2+}$ and $Na^+$ were the dominant ion components with the concentration of 11.3, 7.6, 4.2, and 6.1 μg $m^{-3}$ during the passage of YS, compared to the corresponding concentrations of 4.1, 4.6, 0.4, and 1.1 μg $m^{-3}$ after the passage of YS over Korea. The size-resolved composition in Seoul Korea during the YS event showed a main peak of sulfate in the coarse mode. The YS aerosols transported to Korea were mainly composed of $CaSO_4$ and $Ca(NO_3)_2$ in the coarse mode. A significant amount of $SO_4^{2-}$ and $NO_3^-$ could be formed through the absorption and subsequent conversion of $SO_2$ and NOx on the mineral dust during the long-range transport of Yellow Sand.

It is also found from the Lagrangian model approach that the sulfate formation strongly depends on the mass accommodation coefficient, ambient $SO_2$ concentration, and particle size distribution. Turnover time for $SO_2$ is quite shorter than previous investigations, because the heterogeneous conversion rate is large during the YS event due to high dust loadings. In addition, it is found that $SO_2$ and sulfuric acid deposit onto the coarse mode that provides the large surface area available for deposition. The results show the remarkable increase in sulfate formation with the increase of α , due to fast $SO_2$ transformation to sulfate on the dust particle. During the transport of Yellow Sand, the conversion process of $SO_2$ is more important than the deposition process. However, the accurate value of α is required for the sulfate formation. The information on $SO_2$ and sulfate concentrations in the source region is prerequisite for the estimation of α value.

The advanced program for the well-coordinated measurements will be necessary to obtain a consistent data set for elaborate physical and chemical properties of Yellow Sand at targeted locations such as in the dust source region, in the downstream region, and in the remote marine environment, which could consequently help to understand the characteristics of Yellow Sand. In addition, the relative humidity will be important on the formation of sulfates. Moisture supply over the Yellow Sea should be more carefully investigated into various episodes in the future. Finally, this study should be incorporated into 3-dimensional regional-scale chemical model to shed a light on the complex aerosol dynamic processes.

## REFERENCES


Arao, K., and Y. Ishizaka, Volume and mass of Yellow Sand dust from atmospheric turbidity, *J. Meteorl. Soc. Japan, 64(1)*, 79-93, 1986.

Arimoto, R., R.A. Duce, D.L. Savoie, J.M. Prospero, R. Talbot, J.D. Cullen, U. Tomza, N.F. Lewis, and B.J. Ray, Relatonships among aerosol constituents from Asia and north Pacific during PEM-West A, *J. Geophys. Res., 101(D1)*, 2011-2023, 1996.

Benkovitz C.M., C.M. Berkowitz, R.C. Easter, S. Nemesure, R. Wagener, and S.E. Schwartz, Sulfate over the North Atlantic and adjacent continental regions: Evaluation for October and November 1986 using a three-dimensional odel driven by observational-derived meteorology, *J. Geophys. Res., 99(D10)*, 20725-20756. 1994.

Berge, E., H.A. Jakobsen, A regional scale multi-layer model for the calculation of long-term transport and deposition of air pollution in Europe, *Tellus, 50B*, 205-223, 1998.

Chung, K.Y., Numerical simulations of Yellow Sand events observed in Korea. Ph.D. Thesis. Department of Atmospheric Sciences, Seoul National University, 160pp, 1996.

Dentener, F.J., and P.J. Crutzen, Reaction of $N_2O_5$ on tropospheric aerosols : Impacts on the global redistributions of NOx, $O_3$, and OH, *J. Geophys. Res., 98*, 7149-7163, 1993.

Dentener, F.J., G.R. Carmichael, Y. Zhang, J. Lelieveld, and P.J. Crutzen, Role of mineral aerosol as a reactive surface in the global troposphere, *J. Geophys. Res., 101(D17)*, 22869-22889, 1996.

Fuchs, N.A., and A.G. Sutugin, *Highly Dispersed Aerosols*, Butterworth-Heinemann, 105pp, 1970.

Gao Y., R. Arimoto, R.A. Duce, D.S. Lee, and M.Y. Zhou, Input of atmospheric trace elements and the mineral matter to the Yellow sea during the spring of a low-dust year. *J. Geophys. Res.*, 97, 3767-3777, 1992.

Hanel, G., The properties of atmospheric aerosol particles as a function of the relative humidity at thermodynamic equilibrium with the surrounding moist air, *Adv. Geophys., 19*, 73-188, 1976.

Heikes, B.G., and A.M. Thompson, Effects of heterogeneous processes on $NO_3$, HONO, and $HNO_3$ chemistry in the troposphere, *J. Geophys. Res., 88*, 10883-10895, 1983.

Herring, J.A., R.J. Ferek, and P.V. Hobbs, Heterogeneous chemistry in smoke plume from the 1991 Kuwait oil fires, *J. Geophys. Res., 101*, 14451-14463, 1996.

Iwasaka, Y., M. Yamamoto, R. Imasu, and A. Ono, Transport of Asian dust (KOSA) particles: importance of weak KOSA events on the geochemical cycle of soil particles, *Tellus, 40B*, 494-503.

Jacob, D.J., Heterogeneous chemistry and tropospheric ozone, *Atmos. Environ.,34,* 2131-2159, 2000.

Kim B.-G., J.-S. Han, and S.-U. Park, Transport of $SO_2$ and aerosol over the Yellow Sea, *Atmos. Environ., 35(4)*, 727-737, 2001.

Kim, B.-G., and S.-U. Park, Transport and evolution of a winter-time Yellow Sand observed in Korea, *Atmos. Environ., 35(18)*, 3191-3201, 2001.

KIST (Korean Institute of Science and Technology), A study for the long-range transportair pollutants and environmental cooperation in Northeast Asia (III), *NIER Rep*, 386pp, 1998 (in Korean).

KMA (Korean Meteorological Agency), *Monthly Meteorological Data Report* of January of 1999(in Korean), 1999.

KMA (Korean Meteorological Agency), personal communication, 2001.

Klaic, Z., A lagrangian model of long-range transport of sulfur with the diurnal variations of some model parameters, *J. Appl. Meteorol., 35*, 574-586, 1996.

Maahs, H.G., Kinetics and mechanism of the oxidation of S(IV) by ozone in aqueous solution with particular reference to $SO_2$ conversion in nonurban clouds, *J. Geophys. Res., 88*, 10721-10732, 1983.

Ministry of Environment (MOE) Korea, *Monthly Air Pollution Data Report of January, 1999*(in Korean). 1999.

Murayama T., N. Sugimoto, I. Matsui, K. Arao, K. Iokibe, R. Koga, T. Sakai, Y. Kubota, Y. Saito, M. Abo, N. Hagiwara, H. Kuze, N. Kaneyasu, R. Imasu, K. Asai, K. Aoki, Lidar network observation of Asian dust (Kosa) in Japan, *Proceedings of Optical Remote Sensing for Industry and Environmental Monitoring*, Beijing China, 8-15, 1998.

Nishikawa, M., S. Kanamori, N. Kanamori, and T. Misoguchi, Environmental significance of Kosa aerosol (yellow sand dust) collected in Japan, *Proceedings of the 2nd IUAPPA Regional Conference on Air Pollut.*, Seoul Korea, 35-41, 1991.

Parungo, F., Y. Kim, C. Zhu, J. Harris, R. Schnell, X. Li, D. Yang, X. Fang, P. Yan, X. Yu, M. Zhou, Z. Chen, F. Qian, and K. Park, Asian dust storms and their effects on radiation and climate Part II, *STC Technical Report 2959*, 34pp, 1996.

Peter, L., and D. Easter, Binary homogeneous nucleation as a mechanism for new particle formation in the atmosphere, *Mon. update, 3(3)*, 1-5. 1992.

Rogaski, C.A., D.M. Golden, and L.R. Williams, Reactive uptake and hydration experiments on amorphous carbon treated with $NO_2$, $SO_2$, $O_3$, $HNO_3$, and $H_2SO_4$, *Geophys. Res. Lett, 24*, 381-384, 1997.

Song, C.H., Tropospheric aerosols in East Asia : A model study of the evolution processes of dust and sea salt particles during long range transport, Ph.D. Thesis, Department of Chemical and Biochemical Engineering, University of Iowa, 1999.

Wesley, M.L., and B.B. Hicks, Some factors that affect the deposition rates of sulfur dioxide and similar gases on vegetation, *J. Air Pollut. Control Assoc., 27*, 1110-1116, 1977.

Wexler, A.S., F.W. Lurmann, and J.H. Seinfeld, Modeling urban and regional aerosol - I. Model development, *Atmos. Environ.,28*, 531-546. 1994.

Worsnop, D.R., M.S. Zahniser, C.E. Kolb, J.A. Garner, L.R. Watson, J.M. Van Doren, J.T. Jayne, and P. Davidovits, The temperature dependence of mass accommodation of $SO_2$ and $H_2O_2$ on aqueous surfaces, *J. Phys. Chem., 93*, 1159.-1172, 1989.

Xiao, H., G.R. Carmichael, J. Durchenwald, D. Thorton, and A. Bandy, Long-range transport of SOx and dust in East Asia during the PEM West B experiment, *J. Geophys. Res.,* 102(D23), 28589-28612, 1997.

Zhang, X.Y., R. Arimoto, and Z.S. An, Dust emissions from Chinese desert sources linked to variations in atmospheric circulation. *J. Geophys. Res.,* 102, 28041-28047, 1997.

Zhang, Y., and G.R. Carmichael, The role of mineral aerosol in tropospheric chemistry in East Asia - A model study. *J. Appl. Meteorol., 38*, 353-366, 1999.